Exploring Multivariate Dynamics of Emotions Through Time-Varying Self-Assessed Arousal and Valence Ratings

Andrea Gargano*, *Student Member, IEEE,* Mimma Nardelli*, *Member, IEEE,*
and Enzo Pasquale Scilingo, *Senior Member, IEEE,*

Abstract—Emotions arise from a complex interplay of various factors, including conscious experience, physiological processes, and contextual elements. Although emotions are inherently dynamic processes, this aspect is oftentimes neglected in experimental protocols. In this study, we employed dynamical systems theory to investigate the time-varying self-assessed emotion ratings. We used the continuous ratings of the publicly available CASE dataset, in which thirty individuals rated their level of arousal and valence while watching videos designed to evoke four different emotions. Firstly, we analyzed the univariate dynamics by reconstructing the phase space from the arousal and valence series separately and quantified their regularity and spatial complexity by using three metrics: Fuzzy, Sample, and Distribution Entropy. Then, we combined the arousal and valence series by proposing a novel index, the Multichannel Distribution Entropy (MDistEn), to estimate the complexity of the bivariate phase space. By coupling the two dimensions, we found that MDistEn resulted as an effective marker of fear, showing patterns statistically different from all of the other stimuli (p-value$\leq$0.001). These findings support the investigation of the time-varying dynamics of annotated emotion ratings, as a promising pathway to discriminate the onset of fear-related pathological states.

Index Terms—Affective Computing, fear, arousal, valence, Fuzzy Entropy, Distribution Entropy, multivariate, Multichannel Distribution Entropy.

I. INTRODUCTION

THE investigation of the dynamic nature of human emotions constitutes a pivotal role in emotion science, albeit it has long been overshadowed [1], [2]. An emotional state arises, unfolds, and changes naturally over time. Consequently, investigating the subjective experience of emotions with a focus on its *temporal* dimension yields significant computational insights. This approach reveals critical information that can help identify, model, and recognize emotional states as they occur and evolve.

By taking into account the temporal dimension, several researchers have proposed a dynamical system-based theo-

retical conceptualization of emotions and affects: in music-induced emotions [3]–[5], infant emotional development [6], for psychiatric disorders models of schizophrenia [7], and for the design of cognitive architectures [8]. Particularly, in [3], it is proposed a framework grounded on earlier evidence traced by Russell [9], in which a complex system view of emotions is suggested by identifying the affective dimensions of hedonic tone (i.e., valence) and activation (i.e., arousal) as the two basic emotional state-space coordinates. These two dimensions were intended as parsimonious descriptors of the affective space, onto which discrete emotions can be mapped, as well as interacting emotional driving parameters [4]. A similar approach was adopted in [5], where the researchers collected and analyzed second-by-second evaluations of valence and arousal in music excerpts. According to appraisal theories [2], computational models of emotions have been proposed as processes, involving multiple interacting components over time [10], hence intrinsically considering the very dynamic essence of emotional states.

In the field of Affective Computing, several efforts have been addressed towards investigating the dynamics of physiological time series to reveal useful objective information for emotion recognition tasks [11]–[13]. In particular, nonlinear analysis techniques showed their stunning performances when deployed for the analysis of cardiac [14]–[17] and cortical dynamics [11], [18], [19]. Among the available nonlinear measures quantifying chaos in a physiological dynamical system, spatial complexity and irregularity indexes computed through information-theoretic approaches commonly describe the dynamical behavior of a system in its phase-space domain. To date, these nonlinear measures have proved their effectiveness in differentiating between different cardiac [20]–[23] and emotional states [11], [14], [17], [24].

The dynamic aspect of the self-reported emotional experience has frequently been overlooked in practical terms. This is primarily due to both the lack of proper investigation techniques and the limitations imposed by the available data in the field of emotion discrimination and recognition. When considering the standard pipeline followed in experimental protocols for eliciting affective responses, three key components can be identified: the presentation of stimuli designed to evoke emotions, the self-assessment of the subjective experience, and the acquisition of physiological and/or behavioral data. Specifically, while the presentation of stimuli and the acquisition of physiological or behavioral data are usually

time-varying, the self-assessment of the individual's emotional perception occurs only within a specific time frame after the stimulation session. This assessment is often conducted using self-report questionnaires that employ discrete scales, such as PANAS [25] and SAM [26]. Not only does this approach have some limitations as failing to capture the temporal dynamics of the aroused emotional states, but it also shows the inadequacy of using discrete scales to evaluate the experienced emotions. Recently, several researchers have redirected their focus to novel annotation tools [27], [28] that enable the continuous assessment of emotional perception throughout the process of affective elicitation. The publicly-available Continuously Annotated Signal of Emotion (CASE) dataset [29] was built up by continuous self-assessed annotated ratings of the arousal and valence dimensions, according to Russell's Circumplex Model of Affects [9]. This dataset contains recordings of the annotated self-assessed ratings and physiological signals collected from 30 healthy participants elicited with short emotional videos. In [28], the authors previously reported statistically significant differences in the mean arousal and valence values.

In this study, we used the time-varying annotated signals provided by the CASE dataset for quantifying the complexity of nonlinear emotional dynamics. These time series provided a valuable resource for analyzing continuous self-assessed ratings. Remarkably, the existing literature has not yet highlighted the importance of analyzing and characterizing the complex dynamics of conscious emotional perception using nonlinear time series analysis techniques [30]. Therefore, we aim to provide novel insights by computing synthetic indexes benefiting from the available CASE time-varying scores rather than the discrete ones, usually used in standard protocols for emotion evaluation [16], [31], [32]. Emotions have already been investigated as complex systems [1], [2], and their characterization could benefit from information-theory approaches, such as entropy-based indexes, aimed at quantifying the information content embedded in the temporal dynamics of measured variables. As we preliminary observed in [33], the annotated time-varying arousal ratings show different entropy levels when comparing fear and relaxing stimuli perception. Consequently, the goal of this work lies in delving into the if and how entropy indexes describe different emotion types when accounting for the dynamic behavior of time-varying arousal and valence ratings. In addition, we propose a novel multichannel complexity index, which describes the emotion process in a hybrid and comprehensive manner, taking into account both arousal and valence dimensions.

Specifically, we used Takens's theorem for the phase-space reconstruction [34]. Firstly, we tested the low fractal dimension of the attractors of arousal and valence time series using the correlation dimension method [35]. Then, we applied entropy algorithms (i.e., Sample Entropy (SampEn), Fuzzy Entropy (FuzzyEn) and Distribution Entropy (DistEn) [11], [15], [17], [24]) on the reconstructed phase-space trajectories, decoupling the information in the arousal and valence series by analyzing them separately. Finally, a bivariate analysis was performed by combining the valence and arousal series, proposing a novel approach: the Multichannel Distribution Entropy (MDistEn).

Furthermore, to provide a comprehensive design of the conscious and unconscious aspects of the emotional process, we studied the linear and nonlinear cardiovascular dynamics by analyzing the electrocardiographic (ECG) signals provided by the CASE dataset.

The rest of this work is organized as follows: in Section II, we describe the CASE dataset, the methodological steps to compute the complexity indexes, and the statistical analysis; experimental results are shown in Section IV; and in Section V we discuss them together with their implications.

II. MATERIALS: ANNOTATED AND PHYSIOLOGICAL DATA

A. The Continuously Annotated Signal of Emotion (CASE) Dataset

The CASE dataset is a collection of both physiological and annotated signals gathered from a cohort of 30 young adults (15 females, aged 25.7 ± 3.1 years; 15 males, aged 28.6 ± 4.8 years) while they watched 8 different video clips [28], [29]. The videos were selected from a list of 20 videos [29] following guidelines by previous studies and the outcomes of a preliminary study. They were specifically designed to evoke four distinct emotions in the viewers: relaxation, fear, amusement, and boredom. Two videos were used to induce each emotion, each with a duration ranging from 119 to 197 seconds. During the experimental sessions, each participant viewed the eight videos in a pseudo-randomized order to discard any effects related to presenting the same sequence of stimuli. A two-minute-long blue screen video was displayed to separate two consecutive emotional stimulations (see Fig. 1, top panel).

In comparison with other datasets that offer continuous ratings of emotions [36]–[40], the CASE dataset has the advantage of providing self-assessed ratings of both the valence and the arousal dimensions of the experienced emotion, according to Russell's bidimensional model of affects [9]. In contrast to conventional approaches that rely on mouse-based annotations, CASE dataset participants employed a Joystick-based Emotion Reporting Interface [41], which enabled them the real-time annotation of the valence and arousal dimensions when watching the emotional videos. A training session, consisting of five short videos, made participants familiarize themselves with the annotation task and the user interface prior to the experiment [29]. As shown in Fig. 1 (bottom panel), the graphical interface for emotion ratings was set up on Russell's Circumplex model of affects [9]. Throughout the entire experimental session, a visual display of the participant's annotations was presented on the upper-right corner of the screen. This feature allowed participants to receive real-time feedback on their own annotations. The Self-Assessment Manikin [26] icons were superimposed on the valence-arousal plane to support users with the annotation task. Each participant was able to rate his/her emotional state along the valence and arousal dimensions, in the [0.5, 9.5] range, by moving and/or holding a red pointer in the graphical interface through the joystick (see Fig. 1, bottom).

Furthermore, during the experimental session, the acquisition of the following physiological signals took place [29]: the
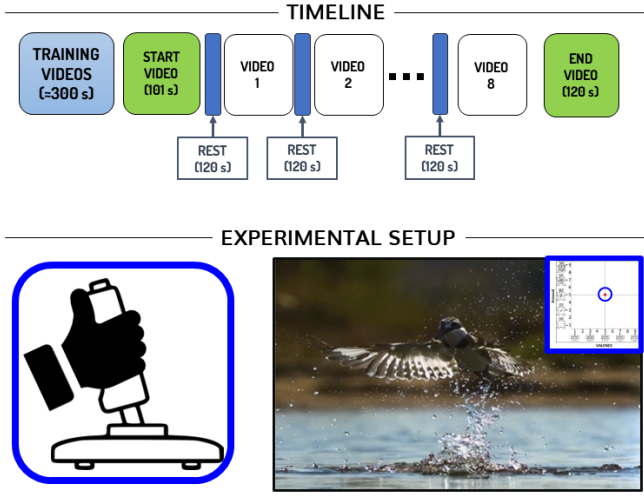
Fig. 1. (Top) Representation of the experimental timeline to collect the annotated data in the CASE dataset. (Bottom) Graphical representation of the joystick interface (left) and a picture of the display with the valence-arousal plane superimposed to the video (right), whose details (the valence-arousal plane and the red pointer) are highlighted in blue. The picture on the right is adapted from [28].

electrocardiogram, the respiration signal, the photoplethysmographic signal, the electrodermal activity, the skin temperature, and the electromyographic signals of three facial muscles. A Data Acquisition (DAQ) system was utilized to acquire both physiological and annotation data, with sampling frequencies of 1000 Hz and 20 Hz, respectively. In this work, we analyzed the linearly interpolated arousal and valence annotation data of all eight emotion-eliciting videos and the interbeat series (hereinafter RR series). The linearly interpolated data were provided in [29] as a convenient data source in which latencies, possibly occurring due to problems in data acquisition and logging, were solved through linear interpolation of the raw data. This process did not alter the original sampling frequency of the physiological and annotation data.

B. RR series Analysis

We analyzed the ECG time series for each participant during each emotional stimulation. As a pre-processing step, we employed the software Kubios HRV [42] (version 2.2) to remove artifacts and ectopic beats from the ECG data. Additionally, the software automatically extracted the R peaks from the ECG, thus obtaining the RR series, which was further resampled at a frequency of 4 Hz. According to [43], for each RR series we computed the following standard time and frequency domain features: mean; standard deviation (STD); root mean square of successive differences (RMSSD) between adjacent RR intervals; percentage of the number of pairs of adjacent RR intervals differing by more than 50 ms (pNN50) over all the RR intervals; power in the low frequency (LF power) and high frequency (HF power) bands; ratio between LF power and HF power (LF/HF ratio); HF in normalized units (HFnorm=HF power/(HFpower + LF power)). In addition, following the methodologies we described in III-C, we computed three nonlinear indexes: SampEn, FuzzyEn, and DistEn.

III. METHODS

Nonlinear dynamical system analysis is extensively used to model systems across biological sciences and engineering. A nonlinear dynamical system changes its state over time and can exhibit chaotic and unpredictable behavior. To study these changes, we use a concept known as *phase space* representation [30], a powerful approach to studying the state trajectory when an analytical approach can not be pursued. It is the case of the annotated and physiological time series investigated in this study. Since we do not dispose of a set of equations to describe the temporal evolution of arousal, valence, and RR series dynamics, we employed the measurements of these variables, as well as their availability in different conditions (i.e., emotional stimuli), using nonlinear time series approaches to reconstruct their phase space. In the following Sections, we describe the methodological steps to compute the correlation dimension and three state-of-the-art entropy indexes commonly used to characterize the phase spaces: Sample Entropy, Fuzzy Entropy, and Distribution Entropy. Moreover, since the objective of this study is to comprehensively characterize the dynamics of emotion processes, we will also delve into the details of the computation of two multichannel entropy indexes encompassing more than one phase space at the same time: Multichannel Fuzzy Entropy and Multichannel Distribution Entropy, the last one being an original contribution of this work.

A. Time-Delay Reconstruction of Phase Space

To analyze the nonlinear dynamics of the annotated ratings of arousal and valence dimensions and the RR series, the starting point was the time-delay reconstruction of phase space. We considered each participant's annotated rating in each video stimulation as a unique time series.

To reconstruct the phase space from a time series we applied Takens's embedding theorem [34], which requires determining two parameters: the time delay (τ) and the embedding dimension (m). The time delay estimates how points in the time series are connected, while the embedding dimension conveys information on the dimensionality of the space we are mapping the time series into. Specifically, we computed τ as the first minimum of the auto-mutual information function [44], through the method described in [45]. Basically, this method takes advantage of kernel density estimation based on standard Gaussian kernels to compute the auto-mutual information, which is defined as the mutual information between the original time series and its delayed version. To scale the variance of the kernel function we selected the smoothing parameters according to Silverman's rule of thumb, which is robust to skew in the distribution of time series data [45]. Regarding the embedding dimension m, we selected its value according to the False Nearest Neighbors algorithm, as originally conceived in [46]. This algorithm requires setting as inputs the τ of the time series being reconstructed and investigating how the number of neighboring points in the phase space trajectory changes when the embedding dimension increases [46].

Starting from the original time series $\underline{x} = [x_1, x_2, \ldots, x_N]$, with N being the overall number of samples, and given the parameters τ and m, we reconstructed the $N - (m-1)\tau$ phase-space vectors in $\mathbb{R}^m$. We computed each embedded vector $\underline{u}_i$ in the phase space as $\underline{u}_i = [x_i, x_{i+\tau}, \ldots, x_{i+(m-1)\tau}]$, with $i \in [1, N - (m-1)\tau]$. The embedded vectors' coordinates defined the states of the arousal and valence dimensions in their phase spaces.

B. Correlation Dimension Analysis

Before applying information-theoretic measures to characterize the annotated time series, we investigated the self-similarity property of these signals. In a general sense, the concept of self-similarity refers to the property of certain objects having the same structure at different scales. When applied to signals, this property manifests if the time series shows long-range temporal correlations when changing the temporal scales of investigation [30]. To this aim, we computed the correlation dimension (CorrDim), an estimate of the attractor's dimension of the underlying dynamical system. This measure, first described in [35], has been widely utilized to effectively differentiate various dynamical behaviors, such as deterministic chaos and random noise. It provides valuable insights into the self-similarity property of time series, as self-similar time series exhibit a non-integer attractor dimension [30].

The CorrDim is estimated by looking at the scaling property of the correlation integral, a measure of the spatial correlation of the attractor, defined as:

$$C(l) = \lim_{N \to \infty} \frac{1}{N^2} \sum_{i=1}^{N} \sum_{j=1, j \neq i}^{N} \mathcal{H}(l - d(\underline{u}_i, \underline{u}_j)) \qquad (1)$$

with $\mathcal{H}$ being the Heaviside step function, $d(\underline{u}_i, \underline{u}_j)$ the value of the euclidean distance between two vectors u_i and u_j, and l a threshold value. For small values of l, the correlation integral shows a power law behavior depending on the CorrDim:

$$C(l) \sim l^D \qquad (2)$$

with the exponent D being the CorrDim.

Practically, since experimental time series are limited by their sample size, the D exponent is usually computed as the derivative of the curve given by $C(l)$ with respect to l in a logarithmic plot. For the computation of the derivative, the number of points to consider (i.e., the scaling range) can be related to the smallest available distance between the embedded vectors, namely l_0. In this study, we used the algorithm proposed in [47] to estimate the CorrDim for each video type's arousal and valence time series. Specifically, to calculate the CorrDim values only, we set the value of τ computed as described in Section III-A, and m in the range $[2, 5]$, given the very short duration of the time series. The length of the scaling range (l/l_0) was set equal to 4, according to the guidelines in [47]. We selected as the most reliable estimate of the correlation dimension the value of d computed by setting the maximum possible m inside the range.

C. Entropy Analysis

The nonlinear dynamics of the reconstructed attractors for arousal, valence, and RR series were characterized using three information-theoretic methods: Sample entropy (SampEn) [48], Fuzzy entropy (FuzzyEn) [49], and Distribution Entropy (DistEn) [21]. SampEn is a widely used measure of irregularity for physiological series, FuzzyEn quantifies regularity based on fuzzy theory, and DistEn is an index that captures the spatial complexity of the dynamical system. Hereinafter we provide a brief overview of these three algorithms.

1) Sample Entropy: The algorithm to compute SampEn [48] was devised to quantify the irregularity of physiological time series dynamics. According to its definition, SampEn is the negative natural logarithm of the conditional probability that two m-dimensional trajectories that are similar remain similar when the value of m is increased by a unit, excluding self-matches from the calculation. SampEn depends on three parameters (τ, m, r), where r represents the threshold to compare the distances between pairs of points belonging to the phase space.

Given the parameters describing the reconstructed phase space, our starting point to compute SampEn was evaluating the point distances between all pairs of points. We calculated the Chebyshev's distance $d(\underline{u}_i, \underline{u}_j)$ accounting for each pair of vectors $\underline{u}_i$ and $\underline{u}_j$, with $i \neq j$ to exclude self-matches, as follows:

$$d(\underline{u}_i, \underline{u}_j) = \max_{k=1,\ldots,m} \{|x_{i+(k-1)\tau} - x_{j+(k-1)\tau}|\} \qquad (3)$$

We employed the values $d(\underline{u}_i, \underline{u}_j)$ to compute $B_i^m(r)$, which represents the average number of times the point distances are lower than the threshold r:

$$B_i^m(r) = \frac{1}{N - m\tau - 1} \sum_{j=1, j \neq i}^{N - m\tau} \mathcal{H}(r - d(\underline{u}_i, \underline{u}_j)) \qquad (4)$$

for $i \in [1; N - m\tau]$, with $i \neq j$ to exclude self-matches and N being the overall length of the original time series. $\mathcal{H}$ is the Heaviside step function. We chose the parameter r as the 20% of the standard deviation of each time series, according to previous literature [48], [50], [51]. We computed the value $B^m(r)$ as follows:

$$B^m(r) = \frac{1}{N - m\tau} \sum_{i=1}^{N - m\tau} B_i^m(r) \qquad (5)$$

with $N - m\tau$ being the total number of vectors. Then, after increasing the embedding dimension value from m to $m + 1$, we computed $B^{m+1}(r)$ according to the procedure pointed out from equation (3) to equation (5). Finally, the SampEn value results from the following equation:

$$SampEn(m, \tau, r, N) = -\ln\left(\frac{B^{m+1}(r)}{B^m(r)}\right) \qquad (6)$$

2) Fuzzy Entropy: In [49], Chen et al. introduced FuzzyEn as a method to assess the regularity of reconstructed phase spaces. FuzzyEn was designed to mitigate the influence of the parameter r on measuring the distances between pairs of points in the phase space. Specifically, it utilizes the concept

of *fuzzy sets* to measure the closeness of points in the phase space by assigning a continuous value between 0 and 1 to each distance between pairs of points based on a *membership degree* function. This means that each distance between points contributes to the estimation of trajectory similarity using its fuzzy measure. In contrast, SampEn relies on a binary comparison between distances of points in the phase space and a specific threshold (see eq. (4)).

The first step of the algorithm to compute the FuzzyEn is the calculation of the Chebyshev distances $d(\underline{u}_i, \underline{u}_j)$ between each pair of embedded vectors $\underline{u}_i$ and $\underline{u}_j$ in the phase space, according to eq. (3). Then, as a membership degree function, the FuzzyEn algorithm uses the exponential function $\exp(-x^n/r)$, which allowed us to compute the similarity degree $D_{ij}^m(n, r)$ of the embedded vectors $\underline{u}_i$ and $\underline{u}_j$ based on the vector distance, as follows:

$$D_{ij}^m(n, r) = \exp(-[d^m(\underline{u}_i, \underline{u}_j)]^n/r) \qquad (7)$$

with m being the embedding dimension; n and r are parameters related to the width and the gradient of the boundary of the exponential function, respectively. We chose r equal to the 20% of the standard deviation of the time series and the parameter n equal to 2, according to previous literature in physiological time series analysis [49]. Then, the sample correlation measure $A^m(n, r)$ is used to compute the value of the similarity degree for all vectors in the space, averaged by the total number of vectors $N - m\tau$, according to the following formula:

$$A^m(n, r, \tau) = \frac{1}{N - m\tau} \sum_{i=1}^{N-m\tau} \left[\frac{1}{N - m\tau - 1} \sum_{i=1, i \neq j}^{N-m\tau} D_{ij}^m(n, r) \right] \qquad (8)$$

Afterwards, we increased the value of the embedding dimension from m to $m + 1$ and we computed the new values of $D_{ij}^{m+1}(n, r)$ and $A^{m+1}(n, r)$ following the formulas in eq. (7) and (8). The FuzzyEn is then defined as the negative natural logarithm of the deviation of $A^m(n, r, \tau)$ from $A^{m+1}(n, r, \tau)$:

$$FuzzyEn(n, r, m, \tau) = -ln(\frac{A^{m+1}(n, r)}{A^m(n, r)}) \qquad (9)$$

3) Distribution Entropy: We computed the DistEn [21] to quantify the spatial complexity of the reconstructed phase space. The DistEn, in comparison to the SampEn and similar to FuzzyEn, uses all the distances between vectors in the reconstructed phase space. However, the DistEn value relies on the computation of a probability density estimate of distances. The robustness of the input parameters and the time series length represents a significant advantage of the DistEn algorithm [21].

Firstly, we computed the Chebyshev distance $d(\underline{u}_i, \underline{u}_j)$ between each pair of points $\underline{u}_i$ and $\underline{u}_j$ in the phase space, without taking into account self-matches (eq. 3). Then, we employed a histogram-based approach to computing the empirical probability density function (ePDF) of all distance values with $i \neq j$. Given that the overall number of bins equals B, we indicated the probability of the distance value falling in each bin with p_b, with $b \in [1, B]$. We set B according to the method proposed by Friedman and Diaconis [52]. For computational purposes, we rounded the value of B to the nearest power of

2. Finally, we calculated the value of DistEn as the Shannon entropy of the ePDF, normalized by the base 2 logarithm of the number of bins, according to the following equation:

$$DistEn(B, m, \tau) = -\frac{1}{\log_2(B)} \sum_{b=1}^{B} p_b \log_2(p_b) \qquad (10)$$

Normalization is performed in order to restrict the computed values of DistEn within the range $[0, 1]$.

Table I summarizes the key features of the three entropy measures used in this study. Specifically, in the first and second columns of Table I, we explicitly outlined two technical features of the algorithms, i.e., the required parameters and the method used to weigh the distances between points in the phase space. In addition, the third and fourth columns point out each approach's main advantages and disadvantages, respectively. The DistEn index is mainly distinguished from the others by the higher stability with respect to parameter settings, accounting for all distances in the phase space, and its global boundedness by definition [21]. Finally, we provided a brief interpretation of each index in the last column. More in detail, the SampEn and FuzzyEn indexes point out similar behaviors of the phase space characteristics derived from the time series, which is its regularity [21], [48], [49]. In contrast, the DistEn gives information about the spatial organization of the phase space and, therefore, was deemed informative of the spatial complexity due to its sensitivity only to the histogram morphology which, in turn, depends on the probability arrangement (i.e., ePDF) of all distances between points in the phase space [21]. Considering that the CASE dataset offers the possibility of studying the temporal transients of emotional perceptions during very different stimuli in terms of arousal and valence, we investigated the performance of such metrics that quantify the regularity and complexity of the system dynamics as significant descriptors of the emotion generation process.

D. Bivariate Entropy Analysis: Multichannel Fuzzy Entropy and Multichannel Distribution Entropy

We performed a nonlinear analysis of the bivariate phase space to analyze the information of both the arousal and the valence time series as two variables of the same system. As for the univariate case, the first step involved time-delay reconstruction. We followed the approach proposed in [23] for the multivariate phase-space reconstruction to compute the Multichannel Complexity Index.

Specifically, before reconstructing each multivariate phase space, we normalized the amplitudes of the two time series by means of the z-score method [23], [53]. For the general case of a *c*-variate process, we defined the vectors in $\mathbb{R}^c$ of time delays $\underline{\tau} = [\tau_1, \ldots, \tau_c]$ and of embedding dimensions $\underline{m} = [m_1, \ldots, m_c]$, in which each k-th entry of the vector corresponds to the parameter related to the original k-th time series ($\underline{x}_k$). We computed the multivariate embedded vectors $\underline{U}_M$ in $\mathbb{R}^M$ as follows:

$$\underline{U}_M(i) = [u_{i,1}, u_{i,2}, \ldots, u_{i,M}] \qquad (11)$$

TABLE I
SUMMARY OF THE CHARACTERISTICS OF EACH ENTROPY INDEX

ENTROPY INDEX	CHARACTERISTICS				
	Parameters	Distance Usage	Advantages	Disadvantages	Interpretation
SampEn [48]	m, τ, r	$\mathcal{H}(r - d_{i,j})$	- stable for $N > 10^m$ - reduces the biases of previous algorithms (e.g. ApEn [48])	- strong sensitivity to m, τ, r parameters; - does not consider all vector distances; - undefined values for short series; - N-dependent range of values	Regularity: - high for noisy series; - intermediate for chaotic and mixed series; - low for periodic series
FuzzyEn [49]	m, τ, r, n	$\exp\left(-d_{i,j}^n/r\right)$	- less dependence on series length; - assign a weight to all vector distances	- sensitivity to m, τ, r, n parameters; - N-dependent range of values	Regularity: high for noisy series; intermediate for chaotic and mixed series; low for periodic series
DistEn [21]	m, τ, B	$ePDF(d_{i,j}, B)$	- stable for short series; - consider all vector distances in the corresponding ePDF; - bounded in the range [0,1]	- sensitivity to m, τ, B parameters	Spatial Complexity: high for chaotic series; intermediate for noisy and mixed series; low for periodic series

$$u_{i,j} = \mathcal{F}(x_{1,(i+(j-1)\tau_1)}, x_{2,(i+(j-1)\tau_2)}, \cdots, \quad (12)$$
$$x_{k,(i+(j-1)\tau_k)}),$$

with $\mathcal{F}$ being the median value of the k samples and $j \in [1, M]$. Since the median of $\underline{m}$ was equal to 3 for both the arousal and valence dimensions of each emotion-inducing video type, we set $M = 3$ for the bivariate analysis. Subsequently, we constructed the vectors $\underline{U}_M(i)$ for $i \in [1, \min_k(N_k - M\tau_k)]$, with N_k being the length of the k-th time series and τ_k its time lag. Then, we calculated the Chebyshev distance $d(\underline{U}_M(i), \underline{U}_M(j))$ between each pair of embedded vectors $\underline{U}_M(i)$ and $\underline{U}_M(j)$ in the bivariate phase space, without accounting for self matches. According to [23], we computed the Multichannel Fuzzy Entropy (MFuzzyEn) starting from the embedded vectors $\underline{U}_M$, as a measure of regularity of the bivariate process. We set the parameter $R = .2 \times \sum_k std(\underline{x}_k)$ and n equal to 2, according to previous literature in the field [23], [49], [53]. However, it was not possible to apply a multiscale approach to MFuzzyEn, which would have provided specific information on the complexity of the multichannel system, as in [23], since the time series analyzed in this study all had an ultra-short duration. For this reason, we propose a new multichannel complexity index based on the calculation of the Multichannel Distribution Entropy (MDistEn) with a single-scale approach. Following this method, the structural complexity of the reconstructed bivariate attractor is quantified by the DistEn value, found by applying the algorithm described in Section III-C3 to the reconstructed bivariate vectors. The Matlab code of the MDistEn algorithm we have developed is publicly available[1].

[1] https://github.com/grgn96/MDistEn/tree/v0.0.1

E. Statistical Analysis

We computed the values of the nonlinear indexes from the arousal and valence ratings and the standard and nonlinear indexes from the RR series, for each participant and for each video stimulation. Then, for each index and for each induced emotion (scariness, amusement, relaxation, and boredom), we averaged the values computed for the two videos. As an example, all the features belonging to the "SCARY" sample resulted from the average of the values of the "scary-1" and "scary-2" videos.

As a first statistical analysis, we compared the CorrDim and the entropy indexes computed from the valence and arousal time series separately. Therefore, we compared the CorrDim, SampEn, FuzzyEn, and DistEn values through a *within-subject* statistical comparison between the four emotions induced by the videos. Then, we performed the statistical comparison of the multivariate measures, thus obtained by coupling the information in the valence and arousal time series. Specifically, we compared the MDistEn and MFuzzyEn values. Again, we performed a *within-subject* statistical comparison between the four emotional stimulations.

In both analyses, for each measure, we applied the non-parametric Friedman test to investigate differences between the medians of the four samples. If a difference was found, we employed the Wilcoxon signed-rank test for paired samples as the multiple comparison test to compare each combination of two groups. We set the statistical significance level at α=0.05 and we applied the Bonferroni correction when testing for multiple comparisons. We used non-parametric statistical tests due to the non-gaussianity of the sample distributions, demonstrated by testing each sample with the Shapiro-Wilk test. The same statistical tests were applied to investigate the differences in the RR series features for the four emotional stimulations.

TABLE II
VALUES OF CORRELATION DIMENSION FOR THE AROUSAL TIME SERIES,
GROUPED BY VIDEO TYPE

Video Type	CorrDim		
	Median	MAD	Integer %
Scary-1	0.842	0.269	0
Scary-2	0.830	0.208	0
Amusing-1	0.845	0.397	0
Amusing-2	0.653	0.386	0
Relaxing-1	0.683	0.300	3.85
Relaxing-2	0.794	0.426	3.85
Boring-1	0.562	0.198	0
Boring-2	0.505	0.326	0

TABLE III
VALUES OF CORRELATION DIMENSION FOR THE VALENCE TIME SERIES,
GROUPED BY VIDEO TYPE

Video Type	CorrDim		
	Median	MAD	Integer %
Scary-1	0.613	0.274	0
Scary-2	0.604	0.277	0
Amusing-1	0.749	0.444	0
Amusing-2	0.485	0.282	0
Relaxing-1	0.439	0.208	4
Relaxing-2	0.500	0.447	0
Boring-1	0.272	0.203	0
Boring-2	0.325	0.280	0

According to the quality of the signals, we performed all the statistical analyses on a sample of 26 participants. We executed all the analyses using Matlab (Release 2021b, Mathworks Inc., Natick, MA).

IV. RESULTS

A. Correlation Dimension

For the correlation dimension, we listed in Tables II and III the median, the median absolute deviation (MAD), and the percentage of integer values (within a tolerance of 0.01) found for the arousal and valence time series, respectively. The median values show a decreasing trend from the fear- and amusement-inducing videos to the relaxing and boring ones, for both the arousal and valence series. Regarding the percentage of integer values, it is 0 for all video types, except for the "relaxing-1" and "relaxing-2" videos exclusively. However, in these cases, the percentages were always lower than 5%. Statistical tests outlined that no significant differences held for the CorrDim values of the arousal data among stimulations (Friedman test $\chi^2(3) = 5.123$, $p = 0.163$), even if a clear trend appears for these values (Fig. 2, left panel). On the other hand, not only there is a similar trend shown by the CorrDim values of the valence data (Fig. 2, right panel), but post hoc analysis (Friedman test $\chi^2(3) = 8.472$, $p = 0.037$) also reveals a significant difference between the scary sample and the boring one ($p = 0.017$). A report of all post hoc tests for the CorrDim of the valence data is available in Table IV.

B. Univariate entropy analysis

1) Arousal: In Fig. 3a we reported the DistEn, SampEn, and FuzzyEn values for the arousal time series of the four video types. A clear decreasing trend is shown for the DistEn

TABLE IV
ADJUSTED *p-values* OF THE CORRELATION DIMENSION FOR THE
VALENCE TIME SERIES, GROUPED BY EMOTION TYPE

Emotion	Amusing	Relaxing	Boring
Scary	1	0.605	0.017
Amusing		1	0.088
Relaxing			1

from the scary to the boring sample (Fig. 3a, left panel). Specifically, the DistEn for the scary videos has a higher median ($\pm$ MAD) value (0.898 ± 0.030) compared to the amusing (0.881 ± 0.033), the relaxing (0.856 ± 0.057), and the boring (0.801 ± 0.046) videos. The outcome of the Friedman test revealed differences among the four samples ($\chi^2(3) = 19.154$, $p = 2.5 \times 10^{-4}$). After correcting the p-values with Bonferroni's method, we found statistically significant differences between the scary and boring ($p \leq 0.001$) and the amusing and boring stimulations ($p = 0.002$).

The SampEn and FuzzyEn median values do not show the same decreasing trend as the DistEn values. The SampEn exhibits a significantly higher median value (Friedman test $\chi^2(3) = 23.769$, $p = 2.8 \times 10^{-5}$) for the amusing (0.413 ± 0.039) videos, compared in decreasing order to the relaxing (0.330 ± 0.087, $p = 0.007$), the scary (0.320 ± 0.036, $p \leq 0.001$), and the boring (0.266 ± 0.071, $p = 0.002$) videos (Fig. 3a, central panel). Similarly, the FuzzyEn presents the highest median value for the amusing (0.302 ± 0.090) videos, followed in decreasing order by the scary (0.263 ± 0.041), the relaxing (0.262 ± 0.065), and the boring (0.181 ± 0.085) videos (Fig. 3a, right panel). However, the only statistically significant differences (Friedman test $\chi^2(3) = 12.831$, $p = 0.005$) are between the scary and boring ($p = 0.048$) and the amusing and boring stimulations ($p = 0.005$).

Table V summarizes the results of the statistical tests among emotion types for the three entropy indexes computed on the arousal series. Moreover, as depicted in summary in Fig. 5 (left panel), for the arousal data the median of the DistEn values peaks toward the scary stimulation while the amusement stimulation achieves the highest values for the metrics of regularity. Boredom shows the lowest values for all metrics among the four emotion categories.

2) Valence: Fig. 3b shows the DistEn, SampEn, and FuzzyEn values for the valence time series of the four video types. As for the arousal data, the DistEn shows a decreasing trend when comparing all stimulations from the scary to the boring (Fig. 3b, left panel). The DistEn computed for the scary videos presents a higher median value (0.859 ± 0.036) compared to the amusing (0.836 ± 0.063), the relaxing (0.811 ± 0.063), and the boring (0.756 ± 0.063) videos. Furthermore, after testing for differences among groups (Friedman test $\chi^2(3) = 17.954$, $p = 4.5 \times 10^{-4}$), post hoc analysis revealed that the scary stimulation is significantly different from the relaxing ($p = 0.028$) and the boring stimulation ($p \leq 0.001$). Also, we found the amusing and boring stimuli to be significantly different ($p = 0.019$). The SampEn values show a similar tendency as the DistEn values (Fig. 3b, central panel), whereas the FuzzyEn values point out a different behavior (Fig. 3b,
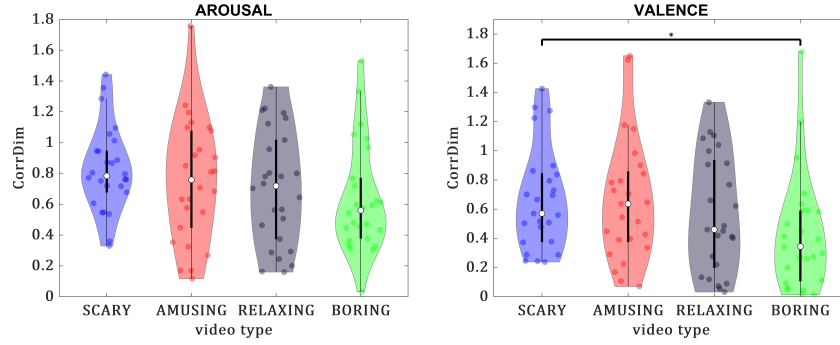
Fig. 2. Violin plots showing the distribution of the CorrDim values for the annotated arousal (left) and valence (right) time series. The values reported here correspond to the average values of the CorrDim, computed by averaging for the same participants the indexes computed from the time series of the two videos (i.e., the two videos for each induced emotion). We reported statistically significant p-values, corrected by the number of multiple comparisons, according to the following legend: * $p \leq 0.050$; ** $p \leq 0.010$; *** $p \leq 0.001$.

TABLE V
ADJUSTED *p-values* OF THE INDEXES FOR THE UNIVARIATE ENTROPY ANALYSIS OF THE AROUSAL TIME SERIES, GROUPED BY EMOTION TYPE

DistEn

Emotion	Amusing	Relaxing	Boring
Scary	1	0.061	3×10^{-4}
Amusing		0.534	0.002
Relaxing			0.451

SampEn

Emotion	Amusing	Relaxing	Boring
Scary	4×10^{-4}	1	1
Amusing		0.007	0.002
Relaxing			1

FuzzyEn

Emotion	Amusing	Relaxing	Boring
Scary	1	1	0.047
Amusing		0.378	0.005
Relaxing			0.187

TABLE VI
ADJUSTED *p-values* OF THE INDEXES FOR THE UNIVARIATE ENTROPY ANALYSIS OF THE VALENCE TIME SERIES, GROUPED BY EMOTION TYPE

DistEn

Emotion	Amusing	Relaxing	Boring
Scary	1	0.028	3×10^{-4}
Amusing		1	0.019
Relaxing			1

SampEn

Emotion	Amusing	Relaxing	Boring
Scary	1	0.356	0.078
Amusing		0.098	0.663
Relaxing			1

FuzzyEn

Emotion	Amusing	Relaxing	Boring
Scary	1	0.335	0.004
Amusing		0.175	0.010
Relaxing			1

right panel), more comparable to the tendency of the FuzzyEn values for the arousal time series. For the SampEn values, we report no statistically significant comparisons (Fig. 3b, central panel), although the Friedman test highlighted group differences ($\chi^2(3) = 10.061$, $p = 0.018$). Conversely, the FuzzyEn values show a higher median value for the amusing videos (0.328 ± 0.065), followed in decreasing order by the scary (0.254 ± 0.070), the relaxing (0.243 ± 0.072), and the boring (0.193 ± 0.062) videos. We found statistically significant differences (Friedman test $\chi^2(3) = 13.338$, $p = 0.004$) between the scary and boring stimulations ($p = 0.004$) and the amusing and boring stimulations ($p = 0.010$) (Fig. 3b, right panel). A summary of the statistical tests among emotion types for the three entropy indexes computed on the valence series is available in Table VI. Moreover, Fig. 5 (central panel) shows a summary of the performances of the metrics for the valence data. As for the arousal data, the DistEn metric appears the best at discriminating the scary stimulation from the other emotion categories (with the only exception of amusement). By contrast, the FuzzyEn peaks toward the amusing stimulation. Boredom achieves the lowest values for all metrics.

C. Bivariate entropy analysis

Fig. 4 shows the MDistEn and MFuzzyEn values for the multivariate analysis based on the valence and arousal time series of the four video types.

The MDistEn values show an almost decreasing trend from the scary to the boring stimulation (Fig. 4, left panel). After testing for differences among the stimulations (Friedman test $\chi^2(3) = 32.908$, $p = 3.4 \times 10^{-7}$), we outlined that the MDistEn values computed for the scary videos present a significantly higher median value (0.834 ± 0.055) compared to the amusing (0.533 ± 0.070, $p \leq 0.001$), the relaxing (0.615 ± 0.091, $p \leq 0.001$), and the boring (0.498 ± 0.077, $p \leq 0.001$) videos. Conversely, for the MFuzzyEn we found an increasing trend when going from the scary to the boring stimulation (Fig. 4, right panel). As for the MDistEn values we found significant differences among groups (Friedman test $\chi^2(3) = 17.031$, $p = 6.9 \times 10^{-4}$). However, the MFuzzyEn values of the scary videos present a significantly lower median value (0.605 ± 0.082) with respect to the amusing (0.771 ± 0.125, $p \leq 0.001$), the relaxing (0.884 ± 0.193, $p = 0.011$), and the boring (0.896 ± 0.179, $p \leq 0.001$) videos.

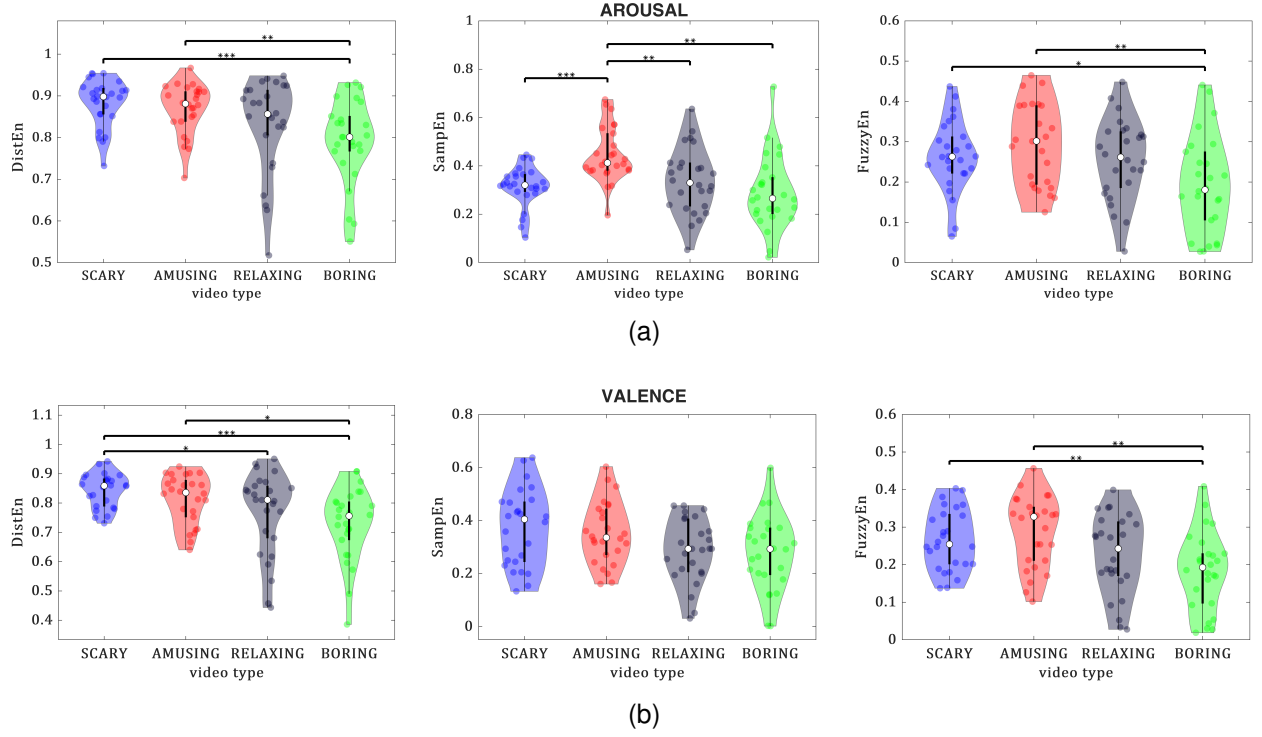In Table VII we reported the post hoc test outcomes for

Fig. 3. Violin plots pointing out the dispersion of the Distribution entropy (DistEn) values (left), the Sample entropy (SampEn) values (center), and the Fuzzy entropy (FuzzyEn) values (right) for the arousal (a) and valence (b) time series annotated during the emotional video stimulations. The values reported here correspond to the averaged values of the entropy indexes, computed by averaging for the same participants the two entropy indexes calculated from the time series of the two videos (i.e., the two videos for each induced emotion). We reported statistically significant p-values, corrected by the number of multiple comparisons, according to the following legend: * $p \leq 0.050$; ** $p \leq 0.010$; *** $p \leq 0.001$.
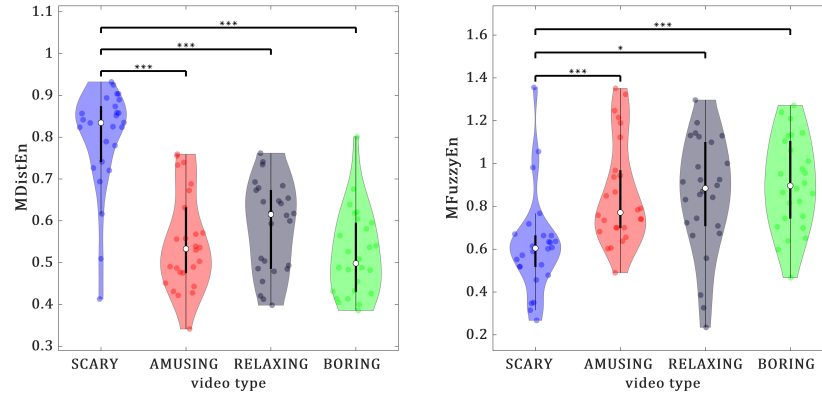

Fig. 4. Violin plots showing the dispersion of the Multichannel Distribution entropy (MDistEn) values (left) and the Multichannel Fuzzy entropy (MFuzzyEn) values (right) for the multivariate analysis of the arousal and valence time series. The values reported here correspond to the average values of the entropy indexes, computed by averaging for the same participants the indexes computed from the time series of the two videos (i.e., the two videos for each induced emotion). We reported statistically significant p-values, corrected by the number of multiple comparisons, according to the following legend: * $p \leq 0.050$; ** $p \leq 0.010$; *** $p \leq 0.001$.

the bivariate entropy analysis. Finally, a summary of the two metrics for the bivariate analysis (Fig. 5, left panel) shows that the MDistEn is picking toward the scary stimulation, with this metric behaving as a clear marker of fearful dynamics. By contrast, the MFuzzyEn peaks toward all the other emotion categories and decreases for the scary one.

D. RR series parameters

Regarding the temporal features, statistical tests highlighted that the median ($\pm$ MAD) value of the mean RR for the scary stimulation (830 ± 84 ms) was significantly lower than the boring one (861 ± 60 ms, $p = 0.011$; Friedman test $\chi^2(3) = 11.400$, $p = 0.010$). Moreover, the STD for the scary stimulation (61 ± 12 ms) was higher than the relaxing one (49 ± 12 ms, $p = 0.018$; Friedman test $\chi^2(3) = 9.923$, $p = 0.019$). For the other temporal parameters, the Friedman test outlined
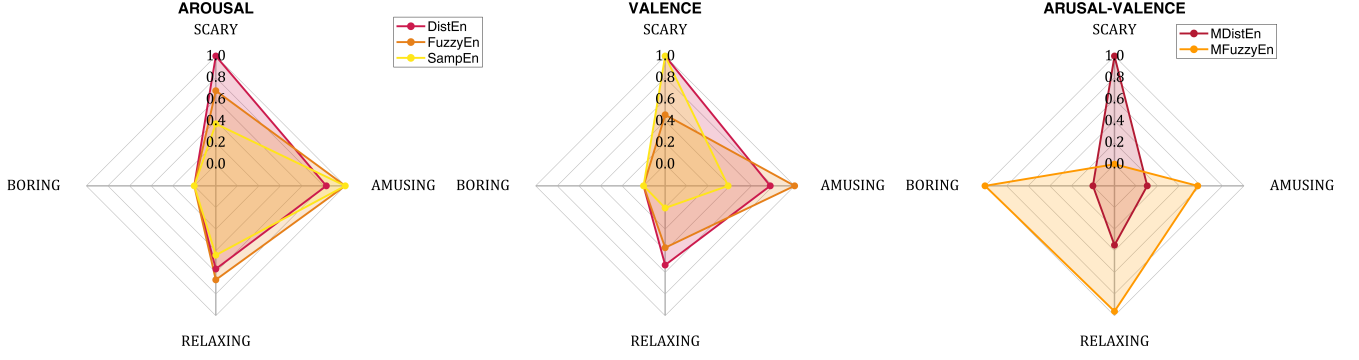
Fig. 5. Radar plots summarizing the capability of each entropy measure to discriminate the four emotion categories (i.e., scariness, amusement, relaxation, and boredom). For each entropy measure, we represented the median of each measure along all emotion categories. Data were normalized in the range [0, 1] through max-min normalization. Plots on the left and at the center show the univariate analysis for arousal and valence, respectively, whereas the plot on the right shows the bivariate analysis.

TABLE VII
ADJUSTED *p-values* OF THE INDEXES FOR THE BIVARIATE ENTROPY
ANALYSIS, GROUPED BY EMOTION TYPE

MDistEn

Emotion	Amusing	Relaxing	Boring
Scary	2.50×10^{-6}	1.97×10^{-5}	1.25×10^{-5}
Amusing		1	1
Relaxing			0.132

MFuzzyEn

Emotion	Amusing	Relaxing	Boring
Scary	2.64×10^{-4}	0.011	9.97×10^{-4}
Amusing		1	0.736
Relaxing			1

TABLE VIII
ADJUSTED *p-values* OF THE RR SERIES PARAMETERS, GROUPED BY
EMOTION TYPE

RR mean

Emotion	Amusing	Relaxing	Boring
Scary	0.261	0.066	0.011
Amusing		0.335	0.123
Relaxing			1

RR STD

Emotion	Amusing	Relaxing	Boring
Scary	0.335	0.018	0.245
Amusing		0.401	1
Relaxing			0.123

LF/HF

Emotion	Amusing	Relaxing	Boring
Scary	0.021	1	1
Amusing		0.663	0.175
Relaxing			1

HF power

Emotion	Amusing	Relaxing	Boring
Scary	0.451	0.296	0.663
Amusing		1	1
Relaxing			1

SampEn

Emotion	Amusing	Relaxing	Boring
Scary	1	0.019	0.356
Amusing		1	1
Relaxing			0.296

no differences among groups for the RMSSD ($\chi^2(3) = 2.815$, $p = 0.421$) and the pNN50 ($\chi^2(3) = 6.190$, $p = 0.103$), respectively.

In addition, for the frequency domain features, the LF/HF ratio showed a significant increase for the amusing stimulation (2.177 ± 0.761) compared to the scary one (1.874 ± 0.693, $p = 0.021$; Friedman test $\chi^2(3) = 9.092$, $p = 0.028$). However, the Friedman test found no differences among groups for the LF power ($\chi^2(3) = 4.846$, $p = 0.183$) and the HFnorm ($\chi^2(3) = 4.754$, $p = 0.191$), respectively. In addition, even if we found group differences for the HF power ($\chi^2(3) = 8.354$, $p = 0.039$), post hoc analysis revealed no differences among specific emotion types after Bonferroni correction.

Finally, the statistical analysis of the nonlinear features pointed out that the SampEn for the scary stimulation (1.102 ± 0.220) was significantly lower than the relaxing (1.334 ± 0.295, $p = 0.019$; Friedman test $\chi^2(3) = 8.215$, $p = 0.042$). We found no differences among groups for the other nonlinear indexes, neither for the FuzzyEn ($\chi^2(3) = 7.246$, $p = 0.065$) nor for the DistEn ($\chi^2(3) = 2.308$, $p = 0.511$), respectively. We reported all adjusted p-values of multiple comparison tests for parameters whose Friedman test rejected H_0 in Table VIII.

E. Summary of Results

We summarize the results reported in Sections IV-A, IV-B, IV-C, IV-D to show several noteworthy findings of this work. Firstly, overall, the CorrDim index showed no significant statistical differences considering the four emotional stimuli for both valence and arousal dimensions, with the only exception being the difference between scary and boring stimuli for the valence series. Results of the univariate entropy analysis, in Section IV-B, reported the same trends for both annotated

dimensions when evaluating the DistEn and FuzzyEn indexes: scary and amusing stimuli resulted to be more complex and irregular than boring. In addition, focusing on the DistEn index, scary stimuli presented significantly higher complexity than relaxing ones along the valence dimension only. By coupling the arousal and valence dimensions and studying the characteristics of the bivariate phase space (Section IV-C), we reported coherent findings, tailored towards a significant difference in fear dynamics compared to the other elicited emotions. Specifically, scary stimuli were found to be the most complex and regular, after statistical analysis. Finally, as outlined in Table VIII, the analysis of the RR series mainly supported our findings on scary stimuli showing a different physiological behavior from other induced emotions: mean RR decreases compared to boring stimulation, RR STD increases and SampEn decreases (i.e., regularity increases) compared to relaxing stimulation.

V. DISCUSSIONS AND CONCLUSION

Previous studies accurately portrayed the importance of accounting for the dynamic nature of human emotions [1], [2], [10]. In the emotion recognition field, the dynamics of physiological signals have been investigated to find objective markers that could aid in the distinction of specific emotions [15], [17] and to understand how affective states influence the dynamics of both the peripheral and central nervous systems [5], [11], [19]. However, to date, very few studies specifically focused on analyzing the conscious perception of emotions [5], [33], with a particular focus on nonlinear dynamics. In this work, to explore the complex dynamics of conscious emotions acquired through a continuous annotation of self-assessed scores in real-time [29], we applied nonlinear time series analysis techniques [30], successfully adopted in previous literature for the analysis of physiological dynamics [11], [15], [17].

We used the time-varying self-assessed arousal and valence ratings of the CASE dataset [29], collected during a protocol of emotion elicitation with eight video clips aiming at inducing four distinct emotions (i.e., scary, amusing, relaxing, and boring). As the first step, we separately reconstructed the phase-space trajectories of the available annotated arousal and valence time series. However, since no empirical knowledge was already available about these annotated data, we estimated the value of their fractal dimension by computing the correlation dimension [35] to ensure the applicability of nonlinear analysis techniques. The correlation dimension values for both series showed very low percentages of having integer values - the latter being a marker of periodic time series [30].

To characterize the trajectories of arousal and valence in the reconstructed phase space, we studied the spatial complexity of their attractors using the DistEn algorithm and quantified their regularity employing the SampEn and FuzzyEn algorithms. Furthermore, we analyzed the cardiac dynamics through the RR series, the most analyzed physiological signal in affecting computing applications [11], [14], [15], [17]. We obtained promising results on each emotion dimension (i.e., arousal and valence), finding similar coherent trends for the DistEn

and FuzzyEn measures. For the arousal and valence data, boredom was less complex and more regular than scariness and amusement, according to the DistEn and FuzzyEn data. However, SampEn partially supported these findings, showing a difference between amusement and all other emotion types, although it was confined to the arousal series alone. Even if the SampEn is recognized as the gold standard measure for time series irregularity, its dependence on signal length was already established and was deemed not suitable for short series [21], [49], [54]. Indeed, since annotated data consist of ultra-short signals, we did not consider the SampEn for further analysis. Finally, we performed a multivariate analysis by combing the valence and arousal data in the bivariate phase space, extracting the MFuzzyEn [23] and applying a novel index: Multichannel Distribution Entropy (MDistEn). More in detail, we employed the approach proposed in [23] to embed the reconstructed trajectories from their different spaces into the same multivariate space, before characterizing the novel dynamics in this new multivariate space. According to this bivariate analysis, the fearful stimulation showed a strikingly different behavior from other emotions, resulting in the most regular and complex emotion type.

Recent works in physiological time series analysis for emotion recognition showed the possibility of reliably modeling fear perception [55], [56]. However, very little is known about the characteristic of the conscious perception of fear when self-rated in an emotion elicitation protocol. Neuroscientific evidence suggests that fear is a complex emotion, not only acting at a conscious level but also nonconsciously, which arises from the interaction of several brain circuits [57]. Indeed, our findings seem to support that, at least at a conscious level, during a fearful video-based elicitation, fear perception appears more complex if compared to other emotions. However, our results support that fear can be partially discriminated from other emotions if accounting for a single emotional dimension only but that the difference always arises when combing the information in both dimensions.

Regarding the cardiac dynamics, we analyzed the RR signal and computed time and frequency domain features, as well as nonlinear ones. According to the time domain analysis, scary elicitation was linked to an increase in heart rate, whereas the amusing clips were reported to be the most arousing stimuli according to LF/HF results. SampEn was the only feature supporting a difference between the scary and the relaxing stimulation, highlighting the more regular dynamics of the RR series during fear-inducing stimuli. This trend found through the nonlinear analysis of physiological signals recalls what we reported by analyzing the entropy of the bivariate arousal-valence attractor according to the MFuzzyEn algorithm [23].

A relevant contribution of this work is the application of the here proposed MDistEn algorithm to characterize the multivariate complexity of annotated time series. This approach, being based on the DistEn algorithm, preserves its crucial advantages [54], such as being parameters-free and showing less dependence on the time series length compared to other multivariate approaches [23]. More specifically, compared to MFuzzyEn [23], the MDistEn metrics inherited an important property from DistEn, namely having normalized values al-

ways belonging to the range [0, 1]. Therefore, it is more suited to effectively compare different processes. For instance, future investigations could establish a subject-dependent cut-off threshold to determine the onset of fear, providing the premises for the use of nonlinear analysis techniques to deepen the understanding of fear-related pathological phenomena, such as anxiety, phobias, and depressive disorders.

The results presented in this work are inherently affected by the length of the inspected annotated signal. Although it is recognized that emotions are short-term affective states, from a signal-processing viewpoint a reasonable balance exists between the length of the analyzed time series and the reliability of the resulting measure. Indeed, we have chosen algorithms whose performances are minimally affected by time series length (i.e., FuzzyEn and DistEn). Future studies should be directed toward lengthy annotated time series collection in emotion-induction protocols. These should be employed to corroborate the validity of our results and investigate the performance of other metrics. In addition, fear was the only emotion with low valence and high arousal provided by the CASE dataset. Future works should extend similar analyses to other emotions, also focusing on more stimuli with comparable expected arousal and valence ratings (i.e., anger, sadness), aiming to validate the specificity of the findings to scary stimuli. In fact, in the case of annotated ratings of emotions with comparable averaged values of arousal and valence, taking into consideration the entire temporal dynamics and quantifying its aspects through dynamical systems theory could bring significant added value. Similar protocols would benefit from recruiting a larger cohort than the currently publicly available dataset, as one of the disadvantages of the CASE dataset is the limited sample size, which inhibits the generalization of findings.

A still unexplored research line envisages the combination of self-assessed conscious emotional experiences (i.e., annotated ratings) and unconscious physiological responses (i.e., physiological signals), aiming at investigating the possible existing linear and nonlinear relationships between them. Investigating linear and nonlinear signal processing approaches of physiological signals and combining these signals with continuous measurements of the conscious emotional experience could disclose still unnoticed psycho-physiological dynamics. Notably, the coupling between the self-assessed conscious experience and the underlying physiological mechanisms holds an impactful potential for novel applications. Accordingly, the use of a similar continuous tracking of emotions in ecological conditions (e.g., out-of-lab) for long-term recordings or affective stimulations with widespread (i.e., smartphones) technologies would favor studying the unknown connections between the dynamics of different emotion-related components - conscious and physiological - which would then foster the prediction of pathological conditions, such as panic, anxiety, and phobias.

REFERENCES

[1] P. Kuppens and P. Verduyn, "Emotion dynamics," *Current Opinion in Psychology*, vol. 17, pp. 22–26, 2017.

[2] K. R. Scherer, "Theory convergence in emotion science is timely and realistic," *Cognition and Emotion*, vol. 36, no. 2, pp. 154–170, 2022.

[3] J. F. Thayer and M. L. Faith, "A dynamic systems model of musically induced emotions," *Annals of the New York Academy of Sciences*, vol. 930, no. 1, pp. 452–456, 2001.

[4] M. Faith and J. F. Thayer, "A dynamical systems interpretation of a dimensional model of emotion," *Scandinavian Journal of Psychology*, vol. 42, no. 2, pp. 121–133, 2001.

[5] O. Grewe, F. Nagel, R. Kopiez, and E. Altenmüller, "Emotions over time: synchronicity and development of subjective, physiological, and facial affective reactions to music." *Emotion*, vol. 7, no. 4, p. 774, 2007.

[6] A. Fogel, E. Nwokah, J. Y. Dedo, D. Messinger, K. L. Dickson, E. Matusov, and S. A. Holt, "Social process theory of emotion: A dynamic systems approach," *Social Development*, vol. 1, no. 2, pp. 122–142, 1992.

[7] G. G. Globus and J. P. Arpaia, "Psychiatry and the new dynamics," *Biological Psychiatry*, vol. 35, no. 5, pp. 352–364, 1994.

[8] R. Jenke and A. Peer, "A cognitive architecture for modeling emotion dynamics: Intensity estimation from physiological signals," *Cognitive Systems Research*, vol. 49, pp. 128–141, 2018.

[9] J. A. Russell, "A circumplex model of affect." *Journal of Personality and Social Psychology*, vol. 39, no. 6, pp. 1161–1178, 1980.

[10] K. R. Scherer, "Towards a Prediction and Data Driven Computational Process Model of Emotion," *IEEE Transactions on Affective Computing*, vol. 12, no. 2, pp. 279–292, Apr. 2021.

[11] J. Marín-Morales, J. L. Higuera-Trujillo, A. Greco, J. Guixeres, C. Llinares, E. P. Scilingo, M. Alcañiz, and G. Valenza, "Affective computing in virtual reality: emotion recognition from brain and heartbeat dynamics using wearable sensors," *Scientific reports*, vol. 8, no. 1, p. 13657, 2018.

[12] J. Shukla, M. Barreda-Ángeles, J. Oliver, G. C. Nandi, and D. Puig, "Feature extraction and selection for emotion recognition from electrodermal activity," *IEEE Transactions on Affective Computing*, vol. 12, no. 4, pp. 857–869, 2021.

[13] E. Kanjo, E. M. Younis, and C. S. Ang, "Deep learning analysis of mobile physiological, environmental and location sensor data for emotion detection," *Information Fusion*, vol. 49, pp. 46–56, 2019.

[14] S. J. Leistedt, P. Linkowski, J. P. Lanquart, J. Mietus, R. B. Davis, A. L. Goldberger, and M. D. Costa, "Decreased neuroautonomic complexity in men during an acute major depressive episode: analysis of heart rate dynamics," *Translational psychiatry*, vol. 1, no. 7, pp. e27–e27, 2011.

[15] M. Nardelli, G. Valenza, A. Greco, A. Lanata, and E. P. Scilingo, "Recognizing emotions induced by affective sounds through heart rate variability," *IEEE Transactions on Affective Computing*, vol. 6, no. 4, pp. 385–394, 2015.

[16] M. Nardelli, A. Greco, M. Bianchi, E. P. Scilingo, and G. Valenza, "Classifying affective haptic stimuli through gender-specific heart rate variability nonlinear analysis," *IEEE Transactions on Affective Computing*, vol. 11, no. 3, pp. 459–469, 2018.

[17] A. Lanata, G. Valenza, M. Nardelli, C. Gentili, and E. P. Scilingo, "Complexity index from a personalized wearable monitoring system for assessing remission in mental health," *IEEE Journal of Biomedical and Health Informatics*, vol. 19, no. 1, pp. 132–139, 2015.

[18] R. Sharma, R. B. Pachori, and P. Sircar, "Automated emotion recognition based on higher order statistics and deep learning algorithm," *Biomedical Signal Processing and Control*, vol. 58, p. 101867, 2020.

[19] B. García-Martínez, A. Martínez-Rodrigo, R. Alcaraz, and A. Fernández-Caballero, "A Review on Nonlinear Methods Using Electroencephalographic Recordings for Emotion Recognition," *IEEE Transactions on Affective Computing*, vol. 12, no. 3, pp. 801–820, Jul. 2021.

[20] M. Costa, A. L. Goldberger, and C.-K. Peng, "Multiscale entropy analysis of complex physiologic time series," *Physical review letters*, vol. 89, no. 6, p. 068102, 2002.

[21] P. Li, C. Liu, K. Li, D. Zheng, C. Liu, and Y. Hou, "Assessing the complexity of short-term heartbeat interval series by distribution entropy," *Medical & biological engineering & computing*, vol. 53, no. 1, pp. 77–87, 2015.

[22] V. Von Tscharner and P. Zandiyeh, "Multi-scale transitions of fuzzy sample entropy of rr-intervals and their phase-randomized surrogates: A possibility to diagnose congestive heart failure," *Biomedical Signal Processing and Control*, vol. 31, pp. 350–356, 2017.

[23] M. Nardelli, E. P. Scilingo, and G. Valenza, "Multichannel complexity index (mci) for a multi-organ physiological complexity assessment," *Physica A: Statistical Mechanics and its Applications*, vol. 530, p. 121543, 2019.

[24] M. Nardelli, A. Greco, O. P. Danzi, C. Perlini, F. Tedeschi, E. P. Scilingo, L. Del Piccolo, and G. Valenza, "Cardiovascular assessment of supportive doctor-patient communication using multi-scale and multi-lag analysis of heartbeat dynamics," *Medical & biological engineering & computing*, vol. 57, pp. 123–134, 2019.

[25] D. Watson, L. A. Clark, and A. Tellegen, "Development and validation of brief measures of positive and negative affect: the PANAS scales," *Journal of Personality and Social Psychology*, vol. 54, no. 6, pp. 1063–1070, 1988.

[26] M. M. Bradley and P. J. Lang, "Measuring emotion: The self-assessment manikin and the semantic differential," *Journal of Behavior Therapy and Experimental Psychiatry*, vol. 25, no. 1, pp. 49–59, 1994.

[27] J. M. Girard and A. G. Wright, "Darma: Software for dual axis rating and media annotation," *Behavior research methods*, vol. 50, no. 3, pp. 902–909, 2018.

[28] K. Sharma, C. Castellini, F. Stulp, and E. L. Van den Broek, "Continuous, real-time emotion annotation: A novel joystick-based analysis framework," *IEEE Transactions on Affective Computing*, vol. 11, no. 1, pp. 78–84, 2020.

[29] K. Sharma, C. Castellini, E. L. van den Broek, A. O. Albu-Schäffer, and F. Schwenker, "A dataset of continuous affect annotations and physiological signals for emotion analysis," *Scientific Data*, vol. 6, 2019.

[30] H. Kantz and T. Schreiber, *Nonlinear time series analysis*. Cambridge university press, 2004, vol. 7.

[31] A. Schaefer, F. Nils, X. Sanchez, and P. Philippot, "Assessing the effectiveness of a large database of emotion-eliciting films: A new tool for emotion researchers," *Cognition and Emotion*, vol. 24, no. 7, p. 1153–1172, Nov. 2010.

[32] M. Nardelli, G. Valenza, A. Greco, A. Lanata, E. P. Scilingo, and R. Bailón, "Quantifying the lagged poincaré plot geometry of ultrashort heart rate variability series: automatic recognition of odor hedonic tone," *Medical & biological engineering & computing*, vol. 58, no. 5, pp. 1099–1112, 2020.

[33] A. Gargano, E. P. Scilingo, and M. Nardelli, "The dynamics of emotions: a preliminary study on continuously annotated arousal signals," in *2022 IEEE International Symposium on Medical Measurements and Applications (MeMeA)*, 2022, pp. 1–6.

[34] F. Takens, "Detecting strange attractors in turbulence," in *Dynamical Systems and Turbulence, Warwick 1980*, D. Rand and L.-S. Young, Eds. Berlin, Heidelberg: Springer Berlin Heidelberg, 1981, pp. 366–381.

[35] P. Grassberger and I. Procaccia, "Measuring the strangeness of strange attractors," *Physica D: nonlinear phenomena*, vol. 9, no. 1-2, pp. 189–208, 1983.

[36] S. Koelstra, C. Muhl, M. Soleymani, J.-S. Lee, A. Yazdani, T. Ebrahimi, T. Pun, A. Nijholt, and I. Patras, "Deap: A database for emotion analysis; using physiological signals," *IEEE transactions on affective computing*, vol. 3, no. 1, pp. 18–31, 2011.

[37] F. Ringeval, A. Sonderegger, J. S. Sauer, and D. Lalanne, "Introducing the recola multimodal corpus of remote collaborative and affective interactions," *10th IEEE International Conference and Workshops on Automatic Face and Gesture Recognition (FG)*, pp. 1–8, 2013.

[38] M. K. Abadi, S. Ramanathan, S. M. Kia, P. Avesani, I. Patras, and N. Sebe, "Decaf: Meg-based multimodal database for decoding affective physiological responses," *IEEE Transactions on Affective Computing*, vol. 6, pp. 209–222, 2015.

[39] F. Ringeval, B. Schuller, M. Valstar, J. Gratch, R. Cowie, S. Scherer, S. Mozgai, N. Cummins, M. Schmitt, and M. Pantic, "Avec 2017: Real-life depression, and affect recognition workshop and challenge," in *Proceedings of the 7th annual workshop on audio/visual emotion challenge*, 2017, pp. 3–9.

[40] J. A. Miranda-Correa, M. K. Abadi, N. Sebe, and I. Patras, "Amigos: A dataset for affect, personality and mood research on individuals and groups," *IEEE Transactions on Affective Computing*, vol. 12, no. 2, pp. 479–493, 2018.

[41] J. Antony, K. Sharma, C. Castellini, E. L. van den Broek, and C. W. Borst, "Continuous affect state annotation using a joystick-based user interface," in *Proceedings of Measuring Behavior 2014: 9th International Conference on Methods and Techniques in Behavioral Research*, 2014, pp. 268–271.

[42] M. P. Tarvainen, J.-P. Niskanen, J. A. Lipponen, P. O. Ranta-aho, and P. A. Karjalainen, "Kubios hrv – heart rate variability analysis software," *Computer Methods and Programs in Biomedicine*, vol. 113, no. 1, p. 210–220, Jan 2014.

[43] Task Force of The European Society of Cardiology and The North American Society of Pacing and Electrophysiology, "Heart rate variability: standards of measurement, physiological interpretation and clinical use," *Circulation*, vol. 93, no. 5, pp. 1043–1065, 1996.

[44] H. D. I. Abarbanel, R. Brown, J. J. Sidorowich, and L. S. Tsimring, "The analysis of observed chaotic data in physical systems," *Rev. Mod. Phys.*, vol. 65, pp. 1331–1392, Oct 1993. [Online]. Available: https://link.aps.org/doi/10.1103/RevModPhys.65.1331

[45] R. D. Thomas, N. C. Moses, E. A. Semple, and A. J. Strang, "An efficient algorithm for the computation of average mutual information: validation and implementation in matlab," *Journal of Mathematical Psychology*, vol. 61, pp. 45–59, 2014.

[46] M. B. Kennel, R. Brown, and H. D. Abarbanel, "Determining embedding dimension for phase-space reconstruction using a geometrical construction," *Physical review. A, Atomic, molecular, and optical physics*, vol. 45, no. 6, pp. 3403–3411, 1992.

[47] D. Kugiumtzis and A. Tsimpiris, "Measures of analysis of time series (mats): A matlab toolkit for computation of multiple measures on time series data bases," *Journal of Statistical Software*, vol. 33, no. 5, p. 1–30, 2010. [Online]. Available: https://www.jstatsoft.org/index.php/jss/article/view/v033i05

[48] J. S. Richman and R. J. Moorman, "Physiological time-series analysis using approximate entropy and sample entropy," *American journal of physiology. Heart and circulatory physiology*, vol. 278, no. 6, p. H2039–H2049, Jun. 2000.

[49] W. Chen, Z. Wang, H. Xie, and W. Yu, "Characterization of surface emg signal based on fuzzy entropy," *IEEE Transactions on neural systems and rehabilitation engineering*, vol. 15, no. 2, pp. 266–272, 2007.

[50] D. E. Lake, J. S. Richman, M. P. Griffin, and J. R. Moorman, "Sample entropy analysis of neonatal heart rate variability," *American Journal of Physiology-Regulatory, Integrative and Comparative Physiology*, vol. 283, no. 3, pp. R789–R797, 2002.

[51] S. M. Pincus and A. L. Goldberger, "Physiological time-series analysis: what does regularity quantify?" *American Journal of Physiology-Heart and Circulatory Physiology*, vol. 266, no. 4, pp. H1643–H1656, 1994.

[52] D. Freedman and P. Diaconis, "On the histogram as a density estimator: L_2 theory," *Zeitschrift für Wahrscheinlichkeitstheorie und verwandte Gebiete*, vol. 57, no. 4, pp. 453–476, 1981.

[53] M. U. Ahmed and D. P. Mandic, "Multivariate multiscale entropy analysis," *IEEE Signal processing letters*, vol. 19, no. 2, pp. 91–94, 2011.

[54] C. Karmakar, R. K. Udhayakumar, and M. Palaniswami, "Distribution entropy (disten): A complexity measure to detect arrhythmia from short length rr interval time series," in *2015 37th Annual International Conference of the IEEE Engineering in Medicine and Biology Society (EMBC)*, 2015, pp. 5207–5210.

[55] A. Baldini, S. Frumento, D. Menicucci, A. Gemignani, E. P. Scilingo, and A. Greco, "Subjective fear in virtual reality: a linear mixed-effects analysis of skin conductance," *IEEE Transactions on Affective Computing*, vol. 13, no. 4, pp. 2047–2057, 2022.

[56] Y.-J. Liu, M. Yu, G. Zhao, J. Song, Y. Ge, and Y. Shi, "Real-time movie-induced discrete emotion recognition from eeg signals," *IEEE Transactions on Affective Computing*, vol. 9, no. 4, pp. 550–562, 2017.

[57] J. E. LeDoux, "Coming to terms with fear," *Proceedings of the National Academy of Sciences*, vol. 111, no. 8, pp. 2871–2878, 2014.